Contents lists available at GrowingScience

Current Chemistry Letters

homepage: www.GrowingScience.com

Preparation of *N*-heterylarenes from the perspective of phenylhydrazine-based green chemistry

Guillermo Penieres-Carrillo[a], Ricardo Alfredo Luna-Mora[a*], Francisco Barrera-Téllez[b], Alejandro Martínez-Záldivar[a], Alicia Hernández-Campos[b], Rafael Castillo-Bocanegra[b], Ana M. R. C. Sousa[c] and Hulme Ríos-Guerra[a*]

[a]*Sección Química Orgánica, Facultad de Estudios Superiores Cuautitlán, Universidad Nacional Autónoma de México, Av. 1 de mayo S/N Cuautitlán Izcalli, CP 54740, Estado de México, México*
[b]*Departamento de Farmacia, Facultad de Química, Universidad Nacional Autónoma de México, CP 04510, Ciudad de México, México*
[c]*Centro de Química, Universidade do Minho, Campus de Gualtar, 4710-057 Braga, Portugal*

C H R O N I C L E

Article history:
Received October 4, 2023
Received in revised form
January 10, 2024
Accepted March 23, 2024
Available online
March 23, 2024

Keywords:
α-Nucleophile
Green chemistry
Hyperconjugation effect
Exo-dig closure reaction
H-bonding effects

A B S T R A C T

Herein, modern green synthesis approaches are studied to assemble *N*-heterylarenes scaffolds via a non-catalyzed intramolecular *5/6-exo-dig* cyclocondensation reaction based on the *in-situ* generation of arenehydrazonopentan-/hexan-2-one. Accordingly, the formation of two *N*-heteryl moieties, pyrazol-1-yl and pyridazin-1(4*H*)-yl, was initially studied. Therefore, appropriate fluorophenyl was first converted into their respective phenylhydrazine by S_NAr reaction and then reacted with different trigonal carbonyl bielectrophiles (–CO–, $–CO_2R$, and $–CO_2H$) in ethanol in the presence of US, MW, IR, and an IR· US irradiation mixture. Cyclic nitrogenous cores were best obtained when subjected to microwave irradiation with ketone and arylhydrazine as starting reagents, allowing them to get excellent yields quickly. Arylhydrazine reactants featuring π-donor groups underwent the best *5/6-exo-dig* type annulment reaction. Presumably, the observed improvements in EDG-dependent reaction efficiency reflect changes in the nucleophilicity of arylhydrazines intermediates as α-nucleophilic reactants.

1. Introduction

Nitrogen-containing heterocycles stand out as one of the most developable privileged scaffolds in the pharmaceutical field.[1] Notably, the pyrazole and pyridazine nuclei have been considered key pharmacophores in searching for and developing novel drugs and drug candidates. Its applications range from pharmacological and agrochemicals to material science. Highlighting that over the past five years, at least twenty-one pyrazole-containing drug candidates have been approved to treat diseases ranging from VIH infections, rheumatoid arthritis, cystic fibrosis, glaucoma to cancer, and cardiac disorders (Fig. 1).[2] Although the 5- and 6-membered nitrogen ring synthetic approaches have been primarily studied, versatile synthesis protocols remain challenging for medicinal and synthetic chemists. To further complicate matters, their synthesis has typically been achieved using acids as catalysts and traditional heat transfer methods, such as heating mantles or oil and sand baths, known as more polluting and less chemically efficient energy sources. To address this issue, our research group has strived to relaunch greener methodologies using combined ultrasound-infrared (USIR), microwave (MW), infrared (IR), and sonochemistry (US) energies as less polluting alternative and more efficient sources capable of conducting reactions in liquid and supported media.[3] Since sustainable approaches have been convincingly shown to dramatically improve environmental issues[4] related to chemistry activities, including reaction time through robust process acceleration, we find it compelling to seek to examine these capabilities to drive the intramolecular closure of *5-exo-dig* of arenehydrazonopentan-/hexan-2-one generated *in situ* from a mixture of phenylhydrazine derivatives and various π carbonyl bielectrophiles to compare their reaction efficiency in obtaining pyrazole and pyridazine nuclei with the thermal approach.

* Corresponding author
E-mail address paulricardo1@yahoo.com.mx (R. A. Luna-Mora) hulmerg@yahoo.com (H. Ríos-Guerra)

doi: 10.5267/j.ccl.2024.3.006

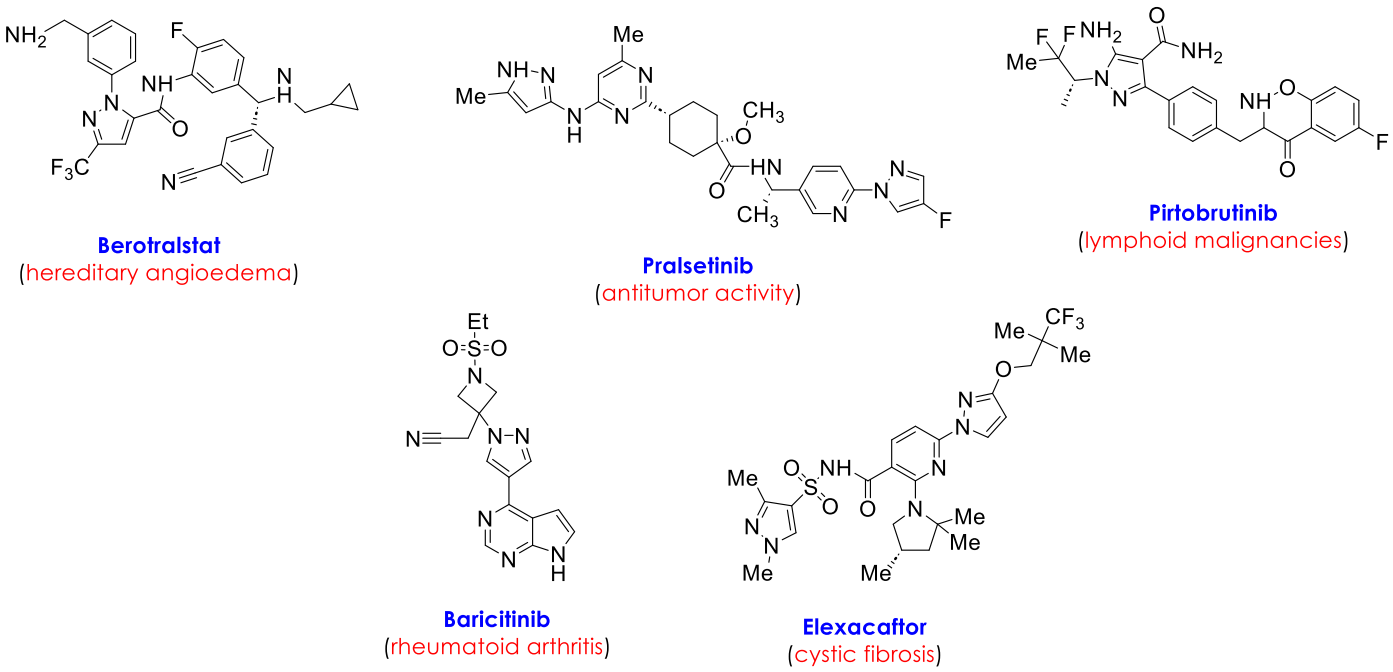

Fig. 1. Selected examples of azaheterocycle scaffolds recently developed in the pharmaceutical sector.

Therefore, given their essential implications regarding synthetic building blocks, reactivity, and our interest in bioactivity cyclic nitrogenous compounds, we sought to synthesize the above *N*-heterylarenes from the catalyst-free phenylhydrazine-based green chemistry perspective, in addition to examining the effect of the solvent on the efficiency of the reaction.

2. Results and Discussion

Although access to azaheterocycles scaffolds such as pyrazole and pyridazine has been extensively reported elsewhere,[5] conventional methodologies that spur *p*-NO_2 arenehydrazine-based *5(6)-exo-dig* type cyclization in the absence of an acidic catalyst are rare and challenging, if at all.[6] Nonetheless, it is known that the efficiency and reaction rate under unconventional conditions can be dramatically improved due to the intrinsic polarizability of the reagents and media of reaction.[7]

Table 1. Protocols examined for the assembly of 2-nitroheterylaniline as a model reaction.

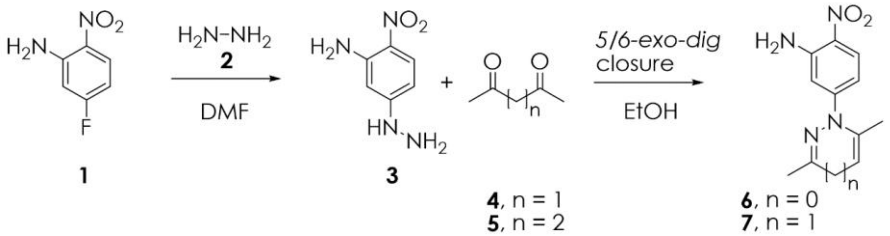

Entry	Product (n)	Source energy* time (h) /yield (%)				
			IR		IR .	
1	**3** (---)	1.50 / 57	3.34 / 46	1.59 / 40	3.00 / 38	0.44 / 62
2	**6** (0)	4.0 / 61	1.5 / 70	2.4 / 51	3.0 / 56	0.116 / 72
3	**7** (1)	4.0 / 60	1.7 / 66	3.6 / 49	3.5 / 52	0.166 / 69

*Thermal: , Infrared: IR, Ultrasound: , Mixture of Infrared-Ultrasound: IR . , and Microwave: .

This intriguing background leads us first to examine the S_NAr reaction between 5-fluoro-2-nitroaniline **1** and monohydrated hydrazine **2**, an ambident nucleophile endowed with α-effect,[8] followed the annulation of the resultant product, 4-nitro-3-aminophenylhydrazine **3**, with bielectrophile carbonyl substrates stimulated with several types of energies (Table 1). By exploiting the S_NAr reaction in DMF, it was clear that at least the IR, US, and USIR energies

examined were not improved in time and yield over the conventional approach (entry 1, Table 1). At best, US irradiation provides comparable results to the orthodox method. However, both offer moderate throughput and more extended time than the MW approach, which is the best. These outcomes suggest that the MW method could be considered a more efficient technique for carrying out S_NAr reactions. We next focused on examining whether *5(6)-exo-dig* type cyclocondensation, which follows the initial nucleophilic addition to carbonyl, could be achieved by reacting **3** as an exceptional α–nucleophile with bielectrophilic carbonyl substrates (entries 2 and 3, Table 1). Preliminary studies using THF, toluene, $CHCl_3$, and DCM as solvents resulted in low yields for converting **3** to heterylaniline **6** (38, 40, 50, and 54%, respectively). However, by switching to EtOH, a protic polar solvent endowed with hydrogen bonding forming effects,[9] the pursued product was accessed in good yield (72%). The solvent-dependent improvement in reaction efficiency suggests significant changes in the electrophilicity of the carbonyl function (endowed with a dielectric nature) due to a cumulative induced net charge arising from the formation of ordered H-bond networks when subjected to an alternating electric field (**Fig. 2**).[10] Therefore, it could be argued that its greater reactivity is connected to the ability to disrupt the π stabilization energy because forming these H-bonds networks additionally imposes an ordered transition state ($\Delta S^{\ddagger}$) that favors the reactive conformers. This built-in electronic effect could be said to reduce the energy of the lowest unoccupied molecular orbital (LUMO) to favor better orbital control. Therefore, carbonyl reactivity is affected by the nature of the energy used and the type of reaction medium imposed. Consequently, the most significant acceleration experienced by the *5/6-exo-dig* intramolecular closure is better revealed when using the MW source because of the decrease in $\pi^*_{C=O}$ orbital energy as the electronic effects are influenced within an ordered network of hydrogen bonds under the influence of an alternating electric field.

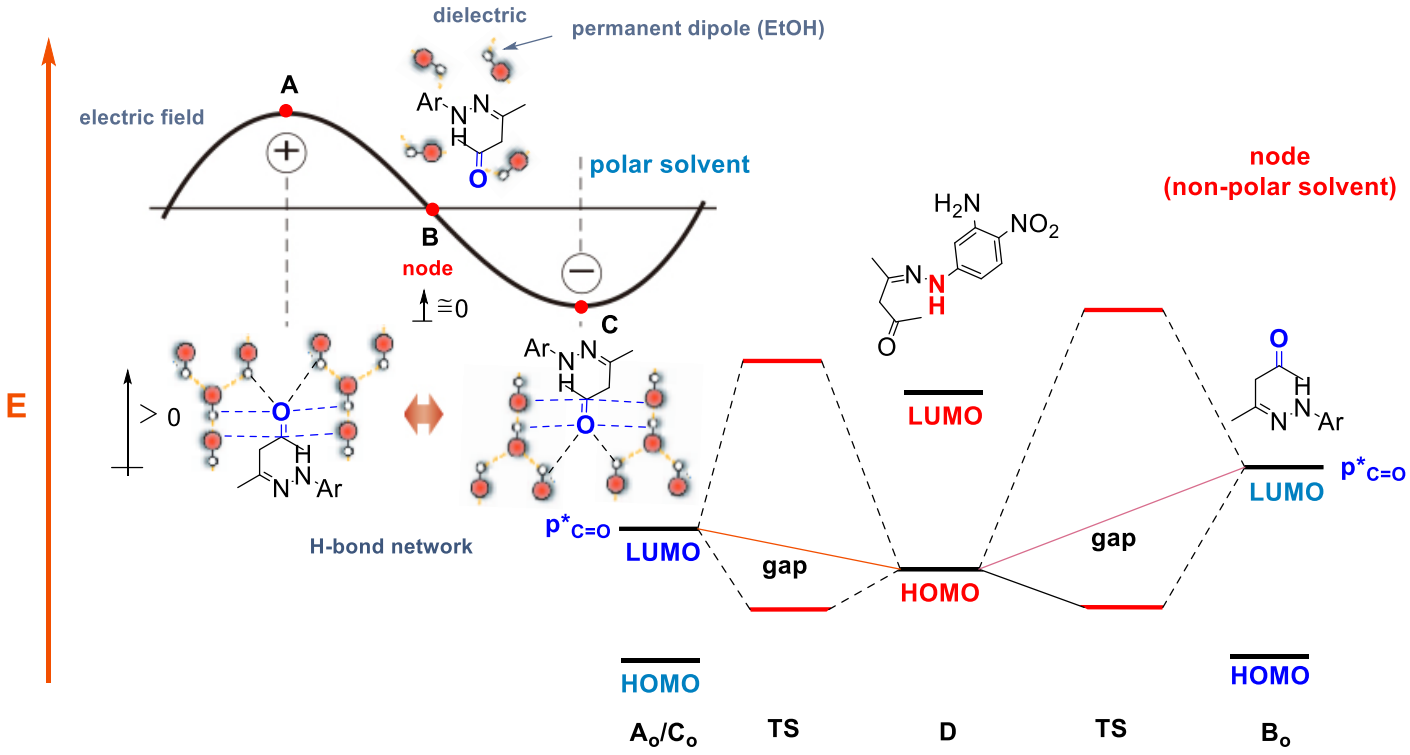

Fig. 2. The greater reactivity of the C=O group when exposed to MW sources could be understood in terms of the magnitude of the strength of the hydrogen bonds generated by ethanol ( )and the negative entropic effect achieved by subjecting it to an alternating electric field (top). Thus, at the maximum amplitude (**A** or **C**), the more significant ethanol-induced polarization upon the C=O brings about decreasing $\pi^*_{C=O}$ orbital energy (LUMO, $\mathbf{A_o/C_o}$) that favors orbital control reactions. This key polar effect becomes negligible at the node point (**B**), where the primarily random arrangement of molecules prevails. This lack of perturbation at the node point (**B**) resembles non-polar solvent effects incapable of generating net polarization, causing an increase in the LUMO energy to the detriment of reaction efficiency (**Bo**).

Therefore, using either β– or γ-dicarbonyl substrates as pentane-2,4-dione **4** or hexane-2,5-dione **5** in EtOH, and in both cases, the azaheterocyclic products (**6**, **7**) were successfully formed in moderate to excellent yields. As in the S_NAr reaction, no substantial yield and reaction time differences were observed between thermal, US, and USIR methods. It should be noted that although IR irradiation significantly influences the improvement of these parameters, the MW method stands out as the best. Despite the good outcomes obtained with the last method, we were intrigued if the overall yield could be improved by increasing the stoichiometry of the α-nucleophile **3** from 1.0 to 3.0 equiv. concerning the β-carbonyl substrate. Such variations showed only an inconsequential improvement of 8% (2.0:80% and 3.0:81%), so they do not justify the wasteful use of large amounts of reagent.

Their spectral parameters adequately identified both products (^{1}H/ ^{13}C NMR, HRMS, and IR). For example, in the IR spectroscopy of product **6**, the characteristic sp^3 NH spectral fingerprints were evident at 3470 and 3358 cm^{-1}, along with the sp^2 CH corresponding to the aromatic moiety at 2098 cm^{-1}. Furthermore, the C–N bond was identified at 1614 cm^{-1}, while the $-NO_2$ motif was confirmed by two observable bands at 1551 and 1213 cm^{-1}. Further analysis of the collected ^{1}H NMR spectral data allowed us to corroborate the presence of the two $-NH_2$ protons bound to the aryl motif shown as a broad singlet at 5.35 ppm. At the same time, the signals for its three aromatic hydrogens were observed at 7.45 (1H, d, J = 2.4 Hz), 7.98 (1H, dd, J = 8.1, 2.4 Hz), and 8.17 (1H, d, J = 8.1 Hz) ppm. Additionally, the singlet for the aromatic hydrogen ascribed to the pyrazo-1-yl aromatic substructure was observed as a singlet at 6.13 ppm, along with the two-methyl signals at 2.18 and 1.94 ppm. In contrast, their respective ^{13}C NMR signals were found in 12.4, 13.2, 106.140.3 and 148.2 ppm. These spectroscopic data agree with the DART [+1] mass spectrum, supporting a peak of *m/z* ratio 232 attributed to the molecular ion with the expected molecular weight and molecular formula $C_{11}H_{13}N_4O_2$.

Encouraged by these appealing initial results, we investigated whether activated phenylhydrazines **3a-f**, which do not embody a strongly electron-withdrawing $-NO_2$ group *para*- to the C_{sp^2}–$NHNH_2$ bond, could be utilized (**Table 2**). In this pursuit, 3-hydrazinylaniline was shown to be an effective coupling partner, providing heterylaniline **8** in an overall yield of 76% (entry 6). Further, arenehydrazines bearing good electron-donating groups (+M) proved to be more effectives in 5-*exo-dig* cyclocondensation (Table 2), and in EtOH, the 5-(3,5-dimethyl-1*H*-pyrazol-1-yl)-2-substitutedaniline (**9-11**, entries 7-9) were formed in near-quantitative yield (91-96%). Notwithstanding, substrates with less electron-withdrawing strength than the NO_2 group also reacted smoothly to give 5-(3,5-dimethyl-1*H*-pyrazol-1-yl)-2-(trifluoromethyl)aniline **12** and 5-(3,5-dimethyl-1*H*-pyrazol-1-yl)-2-isocyanoaniline **13** in 70 and 60% yield (entries 4 and 5, **Table 2**), respectively. These outcomes demonstrate that electron-rich substituents are not necessarily required *para*- to the C_{sp^2}–$NHNH_2$ bond to achieve heterylaniline or heterylbenzonitrile formation successfully.

Table 2. Reaction yields were obtained with *p*-substituted phenylhydrazines with donor- and acceptor-π groups driven by MW irradiation.

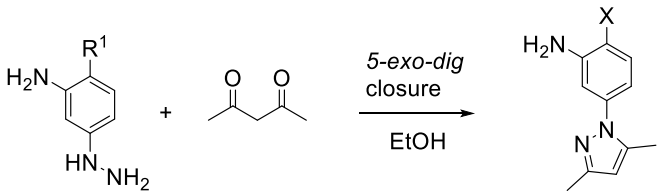

3a-f **4** **8-13**

Entry	Reagent	R^1	Yield (%)	Product
4	**3a**	CF_3	70	**12**
5	**3b**	CN	60	**13**
6	**3c**	H	76	**8**
7	**3d**	Me	91	**9**
8	**3e**	MeO	90	**10**
9	**3f**	NMe_2	96	**11**

To further examine the plausible beneficial effects of green energies on the π energy of the conjugated system on the tethered carbonyl to achieve *exo-dig* closure, other bielectrophilic reagents with more effective π energy stabilizing functionalities were explored. Contrasting results were found when ε–, ζ–dicarboxylic acids, β–, γ–, δ–diesters were input (**Table 3**). Overall, although the best efficiencies and reaction times were achieved with MW irradiation, unfortunately, only the initial acyclic condensation products were isolated **14-18**. These results denote a loss of reactivity toward the intramolecular *exo-dig* closure, leading to the desired *N*-heterylarene, presumably due to the substantial disruption of the α-effect in the N2 atom of acyclic products because of key conjugative and hyperconjugation interactions coming into effect at the two π-acceptor motifs tethered on N1 atom. Accordingly, the α-effect seems to "override" the pure electronic effect (+M/-I) of the 4-nitro-3-aminophenyl moiety on N2, raising the HOMO energy of the N1 atom to make it a better nucleophile. On the contrary, the thermodynamical stability of the resulting acyclic product is related to multiple stabilizing effects, highlighting the disruption of the effect on the N2 atom of the hydrazonyl moiety. Presumably due to the efficient π-conjugation between its lone pair of electrons with the π-orbitals on the phenyl bearing a strong π acceptor group in *para*– position, in addition to hyperconjugative interactions that come into play in the amide moiety, combined with strong stereoelectronic effects (neutral hyperconjugation) that deactivate the electrophilic reactivity of the attached ester or carboxylic by strong interactions with the O lone pairs. Therefore, these changes, like the bound π acceptors moieties, turn off *exo-dig* closure, even though this substructure overcomes the entropic penalty. **Fig. 3** illustrates that this critical deactivation (stabilization) arises from the stereoelectronic effect,[11] mainly the $n_O \rightarrow \pi^*_{CO}$ hyperconjugation effect. Due to this neutral hyperconjugation effect, the LUMO energy of carbonyl of the ester or carboxylic acid increases more than of ketone, making them less susceptible to undergoing a nucleophilic intramolecular closure reaction as might be expected. This means that the activation energy required to disrupt π stabilization is lower

for the ketone ΔE_R and higher for the ester ΔE_{OR} and carboxylic function ΔE_{OH} in the *exo-dig* closure step. Therefore, it is noteworthy that, regardless of the type of energy applied, none could disrupt the strong hyperconjugation effect prevailing in the π-acceptor carbonyl units, which ultimately defines the key reactivity.

Table 3. The yield obtained from the condensation reaction of **3** with carbonyl reagents having more effective conjugated π energy driven under thermal and green energy.

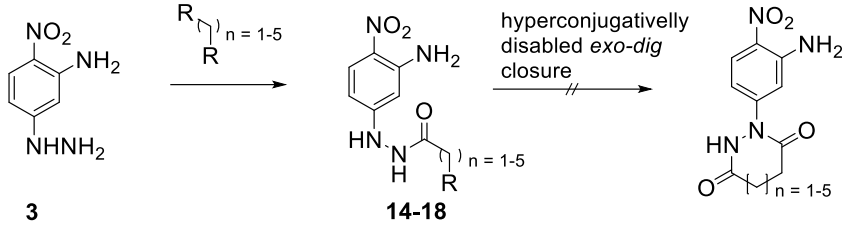

Entry	Product	R (n)	Source energy* time (h) /yield (%)				
			⏀	IR	●	IR · ●	)))
10	**14**	CO_2Et (1)	3.0 / 51	2.5/62	3.3 / 49	2.5 / 56	0.116/ 65
11	**15**	CO_2Et (2)	3.5 / 48	2.5/58	4.0 / 37	2.7 / 60	0.116/ 64
12	**16**	CO_2Et (4)	3.5 / 46	2.5/63	5.0 / 39	3.5 / 59	0.133/ 65
13	**17**	CO_2H (3)	4.6 / 51	2.5/61	5.0 / 38	3.5 / 50	0.166/ 65
14	**18**	CO_2H (5)	4.6 / 45	2.5/58	5.3 / 37	3.7 / 61	0.200/ 66

*Thermal: ⏀, Infrared: IR, Ultrasound: ●, Mixture of Infrared-Ultrasound: IR · ●, and Microwave:))).

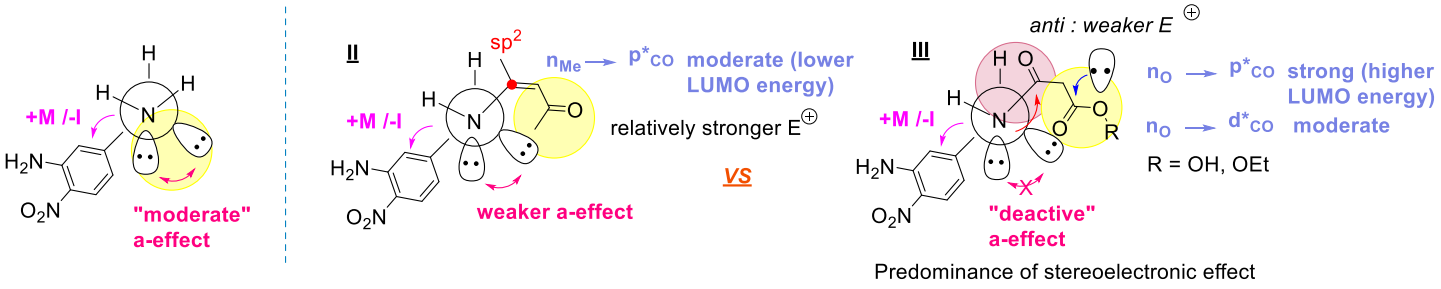

Fig. 3. The stereoelectronic features of oxygen and nitrogen define key reactivity trends, as lone pairs of these atoms engage in strong conjugative and hyperconjugative interplays.

After examining the efficiency of the four green irradiation techniques on the failed *exo-dig* closure process, it was evident that the MW approach spurs better acyclic byproduct reaction efficiency (64-66%) along with faster reaction times. This chemical transformation appears independent of the π nature of the carbonyl group involved in the reaction, even if they are strongly stabilized carboxylic acids (entries 13-14, Table 3). In contrast, the IR technique provides experimentally comparable yields (58-62%) in 2.5 h. Meanwhile, the US approach gets worse in both time and performance. In this regard, the combinatorial effect of IR·US irradiation does not seem to give rise to a synergistic effect, although it does improve compared to US irradiation. After all, the latter type of energy turns out even worse than the thermal method in stimulating condensation reaction between arenephenylhydrazine and π-accepted functionalities.

3. Conclusion

Although microwave energy stood out as a powerful synthetic tool to efficiently drive catalyst-free *exo-dig* closure and S_NAr reactions, overall, most of the alternative heating techniques outperformed conventional methods in terms of efficiency, reaction time, and minimization of environmental impacts. Furthermore, under the specific reaction conditions studied, it was found that the stereoelectronic effects (neutral hyperconjugation) and the reaction medium also define the key trends of chemical reactivity. This means that although the intrinsic nature of the irradiation alone could influence the efficiency of the reaction, the subtle structural changes associated with the nature of the solvents are decisive. Nonetheless, it should be noted that each technique has its advantages and limitations, so the choice of the most appropriate technique will depend on factors such as the availability of the equipment, the nature of the target compounds, and the specific objectives of the planned project.

Acknowledgments

A very special thank you to my brother Luis Alberto Luna Mora, for the support provided for the transcription of the notes of this work and for the editions provided תודה רבה אח שלי. José G. Penieres-Carrillo and Ricardo A. Luna-Moraacknowledge to DGAPA-UNAM the financial support to PAPIIT IN218515 and FES Cuautitlán-UNAM PIAPI1618 and DGAPA-UNAM PAPIME PE209518 programs. Ricardo A. Luna-Mora thanks to CONACYT for the Grant 32841.

4. Experimental

4.1. Materials and Methods

All reagents and solvents were of commercial quality, obtained from Sigma-Aldrich, and used without further purification. Analytical TLC and preparative chromatography were performed using precoated Kieselgel 60F254 plates and Gel slice MN-Kieselgel G/UV254 plates, respectively. UV (254 nm) was used to visualize the spots. Melting points were determined using a Buchi B-450 melt-point apparatus. ^{1}H and ^{13}C NMR spectra were recorded on a Varian 300 MHz spectrometer, using either $CDCl_3$ or DMSO-$_{d6}$ as solvents. Chemical shifts (δ) are reported in ppm relative to $Si(Me)_4$. Coupling constants *J* are given in Hertz, and the splitting patterns are indicated as singlet (s), doublet (d), triplet (t), or multiplet (m). Mass spectra (MS) and high-resolution mass spectra (HRMS) were obtained using a JEOL Accu TOF JMST100LC spectrometer, using the direct analysis in real time (DART) method. IR spectra were recorded on a Perkin-Elmer 283B spectrophotometer using ATR techniques.

Note: Working with nitrocompounds in microwaves carries its risks, since nitrocompounds tend to be somewhat unstable and energetic, posing a risk of explosion when polynitrated. In our case it was a mononitrated derivative, so its use was considered safe. For more details, review the most recent literature.[12]

4.1.2. Experimental equipment

4.1.2.1. US·IR coupling

The US-IR coupling setup consists of two independent devices: a custom-built IR device equipped with a THERA-TERM OSRAM 250-W Red IR bulb (125 V), emitting a wavelength of 1100 nm (9.09 cm^{-1}) and a thermostat for power output regulation. This homemade device was assembled with A Cole Parmer 500-W 20 kHz ± 50 Hz ultrasonic processor, as shown in supporting information. The IR lamp was positioned approximately 15 cm away from the reaction flask during the reactions, while the ultrasonic horn was placed at about 1.4 cm within the reaction system. The US equipment was set at 80% power and 50% amplitude, with an irradiation frequency of 20 kHz ± 50 Hz. The reaction temperature was monitored using an InfraPro IR thermometer.

4.1.2.2. Ultrasound

A 500-W 20 kHz ± 50 Hz Cole Parmer ultrasonic processor operating at 120 VAC was used in its standard configuration. The reaction temperature was monitored using an InfraPro IR thermometer.

4.1.2.3. Infrared

A homemade electric metallic cylinder 29.5 cm in length and 15.3 cm in width was explicitly designed to hold and place an IR-emitting bulb safely. The bulb used in this setup was a THERA-TERM OSRAM 250-W Red IR bulb, operating at 125 V and emitting a wavelength of 1100 nm (9.09 cm^{-1}). The device has a varicap diode to regulate the output power precisely. The reaction temperature was monitored continuously using an InfraPro IR thermometer. See the supporting information for a visual representation of the apparatus.

4.1.2.4. Microwave

A standard configuration of the Anton Parr monowave synthesis reactor, operating at 300 MW, was used for the experiments. All reactions were performed in sealed microwave vials with a capacity of 20 mL. The reaction temperature was monitored using an immersing ruby thermometer.

4.2. General procedure

*4.2.1 Obtention of 4-nitro-3-amino-phenylhydrazine (**3**)*

In a 50 mL flask, 1 mmol of **1** and 4 mmol of **2** were dissolved in 25 mL of DMF. The mixture was heated to a temperature of 90 °C and subjected to the appropriate energy type and reaction time described in Table 1. The progress of the reactions was followed by TLC. After the reaction time, the crude product was cooled and poured into vigorously stirred ice water. The resulting precipitate was collected, dried, and purified by preparative chromatography using a 6:4 hexane/AcOEt elution system.

*4.2.2 General procedure for the synthesis of (**6-18**)*

In a 20 mL round-bottomed flask containing 10 mL of ethanol, 2 mmol of **3** and 2 mmol of the corresponding dicarbonylic substrate were placed. The mixture was irradiated with the appropriate type of energy, maintaining the temperature at 90 °C for the reaction time described in **Tables 2-3**. TLC followed the progress of the reactions. After concentrating the crude reaction to half the volume, the precipitates were purified using preparative chromatography with hexane/ethyl acetate (6.5:3.5, v/v) as the eluent phase. Only physical data for a few selected compounds are included here.

4.3 Physical and Spectral Data

*4.3.1 5-hydrazinyl-2-nitroaniline (**3**)*. Yield 80%; mp 182 °C; IR (ATR): 3470, 3358 (NH), 1699 (NHC=O), 1614 (CN), 1572, 1366 (NO_2), 962, 897, 802 ($Ar_{1,2,4}$-subst) cm^{-1}; ^1H NMR (300 MHz; DMSO-*d6*/TMS): δ 2.16 (s, 3H), 3.07 (s, 3H), 4.41 (t, *J* = 6.0 Hz, 1H); 6.56 (dd, *J* = 7.2, 2.4 Hz, 1H), 7.61 (d, *J* = 2.4 Hz, 1H), 8.02 (d, *J* = 9.6 Hz, 1H), 10.60 (s, 1H); ^{13}C NMR (75 MHz, DMSO-*d6*/TMS): δ 22.7, 25.4, 102.4, 107.6, 126.6, 128.4, 136.8, 155.0, 169.5, 169.6. HRMS (DART [+1]) Found: 169.06451, calcd for $C_6H_8N_4O_2$: 169.06475.

*4.3.2 5-(3,5-dimethyl-1H-pyrazol-1-yl)-2-nitroaniline (**6**)*. Yield 72%; mp 183-185 °C; 3491, 3377 (NH), 3084, 2956, 2925, 2856 (CH's), 1625 (CN), 1556, 1319 (NO_2), 790, 684 (sust $_{1,2,4}$) cm^{-1}; ^1H NMR (300 MHz; DMSO-*d6*/TMS): δ 1.94 (s, 3H, H_7), 2.18 (s, 3H, H_6), 5.35 (s, 2H, H_{14}, NH_2), 6.13 (s, 1H, H_4), 7.45 (d, 1H, H_9, *J* = 2.4 Hz), 7.98 (dd, 1H, H_{13}, *J* = 8.1 Hz, *J* = 2.1 Hz), 8.17 (d, 1H, H_{12}, *J* = 8.1 Hz). ^{13}C NMR (75 MHz, DMSO-*d6*/TMS): δ 12. 4 C7, 13.2 C6, 99.2 C9, 106.1 C_4, 108.5 C_{13}, 121.3 C_{12}, 130.0 C_{11}, 140.3 C_5, 147.6 C_{10}, 148.2 C_8, 148.7 C_3. HRMS (DART [+1]) Found: 232.09620, calcd for $C_{11}H_{13}N_4O_2$ 232.09600.

*4.3.3 5-(3,6-dimethylpyridazin-1(4H)-yl)-2-nitroaniline (**7**)*. Yield 69%; mp 126-129 °C; 3314, 3239 (NH), 3039,2978, 2966, 2934, 2904, 2851, 2813 (CH's), 1650 (CN), 1525, 1358 (NO_2), 873, 687 (sust $_{1,2,4}$) cm^{-1}. ; ^1H NMR (300 MHz; DMSO-*d6*/TMS): δ 1.96 (s, 1H, H_4), 2.05 (s, 3H, H_7, CH_3), 2.21 (s, 3H, H_8, CH_3), 4.8 (t, 2H, H_5, *J* = 1.4 Hz), 6.75 (s, 1H, H_{10}), 6.80 (d, 1H, H_{14}, *J* = 8.7 Hz), 7.00 (s, 2H, H_{15}, NH_2). ^{13}C NMR (75 MHz, DMSO-*d6*/TMS): δ 9.8 C_7, 11.1 C_8, 30.7 C_4, 97.2 C_5, 102.9 C_{14}, 103.9 C_{10}, 126.9 C_{12}, 130.7 C_{13}, 139.8 C_6, 148.6 C_{11}, 148.9 C_9, 150.2 C_3. HRMS (DART [+1]) Found: 247.111705, calcd for $C_{12}H_{14}N_4O_2$ 247.11680.

*4.3.4 Ethyl 3-(2-(3-amino-4-nitrophenyl)hydrazinyl)-3-oxopropanoate (**14**)*. Yield 69%; mp 175-178 °C; 3288 (NH), 2980, 2939, 2690 (CH's), 1732, 1707 (C=O), 1624 (CN), 1529, 1349 (NO_2), 881, 673 (sust $_{1,2,4}$) cm^{-1}. ^1H NMR (300 MHz; DMSO-*d6*/TMS): δ 1.14-1.19 (m, 3H, H_{14}, CH_3), 3.45 (s, 2H, H_2, *J* = 3.6 Hz), 3.60 (s, 2H, H_{12}, NH_2), 4.10 (q, 2H, H_{13}, *J* =6.3 Hz), 7.43 (s, 1H, H_7), 7.53 (d, 1H, H_{11}, *J* =7.8 Hz), 7.73 (d,1H, H_{10}, *J* = 7.8 Hz), 9.01 (s, 1H, H_5, NH) 10.65 (s, 1H, H_4, NH). ^{13}C NMR (75 MHz, DMSO-*d6*/TMS): δ 13.9 C_{14}, 41.2 C_2, 60.8 C_{13}, 99.2 C_7, 100.2 C_{11}, 120.7 C_9, 130.3 C_{10}, 147.0 C_8, 148.3 C_6, 169.7 C_1, 170.0 C_3. HRMS (DART [+1]) Found: 283.09660, calcd for $C_{11}H_{14}N_4O_5$ 283.09640.

*4.3.5 Ethyl 4-(2-(3-amino-4-nitrophenyl)hydrazinyl)-4-oxobutanoate (**15**)*. Yield 64%; mp 177-179 °C; 3488, 3468, 3363, 3345 (NH), 3092, 3065, 2957, 2926, 2857 (CH's), 1725 (C=O), 1636 (CN), 1568, 1376 (NO_2), 838, 684 (sust $_{1,2,4}$) cm^{-1}. ^1H NMR (300 MHz; DMSO-*d6*/TMS): δ 1.16 (t, 3H, H_{15}, *J* = 7.2 Hz), 2.22 – 2.31 (m, 4H, $H_{2,3}$) 3.54 (s, 1H, H_6, NH), 4.03 (t, 2H, H_{14}, *J* =7.1 HZ), 7.43 (d, 1H, H_8, *J* = 1.8 Hz), 7.56 (d, 1H, H_{12}, *J* = 8.1 Hz), 7.74 (d, 1H, H_{11}, *J* = 8.4 Hz), 9.01 (s, 1H, H_5, NH), 10.63 (s, 2H, H_{13}, NH_2). ^{13}C NMR (75 MHz, DMSO-*d6*/TMS): δ 14.1 C_{15}, 32.2 C_2, 32.8 C_3, 59.7 C_{14}, 100.2 C_8, 104.3 C_{12}, 120.7 C_{10}, 130.3 C_{11}, 146.9 C_9, 150.7 C_7, 171.8 C_1, 172.5 C_4. HRMS (DART [+1]) Found: 296.11223, calcd for $C_{12}H_{16}N_4O_5$ 296.11207.

*4.3.6 Ethyl 6-(2-(3-amino-4-nitrophenyl)hydrazinyl)-6-oxohexanoate (**16**)*. Yield 65%; mp 161-163 °C; 3445, 3347, 3227 (NH), 2955, 2926, 2856 (CH's), 1727 (C=O), 1605 (CN), 1500, 1379 (NO_2), 858, 693 (sust $_{1,2,4}$) cm^{-1}. ^1H NMR (300 MHz; DMSO-*d6*/TMS): δ 1.15 (t, 3H, H_{17}, *J* = 7.2 Hz), 1.25 (sex, 2H, H_4, *J* = 7.5 Hz), 1.47 (sex, 2H, H_3, *J* =7.2 Hz), 2.15 – 2.30 (m, 4H, $H_{2,5}$), 3.6 (s, 1H, H_8, NH), 4.02 (q, 2H, H_{16}, *J* = 7.2 Hz), 7.41 (s, 1H, H_{10}), 7.53 (d, 1H, H_{14}, *J* = 8.1 Hz), 7.75 (d, 1H, H_{13}, *J* =8.1 Hz). ^{13}C NMR (75 MHz, DMSO-*d6*/TMS): δ 14.1 C_{17}, 24.2 C_3, 28.1 C_4, 33.5 C_2, 38.6 C_5, 59.7 C_{16}, 99.2 C_{10}, 100.2 C_{14}, 120.7 C_{12}, 130.3 C_{13}, 146.9 C_{11}. HRMS (DART [+1]) Found: 325.14352, calcd for $C_{14}H_{20}N_4O_5$ 325.143300.

*4.3.7 5-(2-(3-amino-4-nitrophenyl)hydrazinyl)-5-oxopentanoic acid (**17**)*. Yield 65%; mp 172-174 °C; 3470, 3345 (NH),

3064, 2936, 2866 (CH's), 1692 (C=O), 1620 (CN), 1569, 1323 (NO_2), 838, 695 (sust $_{1,2,4}$) cm^{-1}. ^1H NMR (300 MHz; DMSO-$_{d6}$/TMS): δ 1.67 (q, 2H, H_3, J = 7.8 Hz), 2.21 (t, 4H, $H_{2,4}$, J = 7.5 Hz), 7.18 (s, 4H, $H_{6,7,14}$, NH_2, NH, NH), 7.38 (s, 1H, H_9), 7.53 (d, 1H, H_{13}, J = 8.4 Hz), 7.73 (d, 1H, H_{12}, J = 8.4 Hz), 10.61 (s, 1H, H_{15}, OH). ^{13}C NMR (75 MHz, DMSO-$_{d6}$/TMS): δ 20.1 C_3, 30.7 C_2, 32.9 C_4, 99.2 C_9, 100.2 C_{13}, 120.9 C_{11}, 130.4 C_{12}, 147.0 C_{10}, 148.8 C_8, 172.9 C_5, 174.4 C_1. HRMS (DART [+1]) Found: 283.09642, calcd for $C_{11}H_{14}N_4O_5$ 283.09977.

*4.3.8 7-(2-(3-amino-4-nitrophenyl)hydrazinyl)-7-oxoheptanoic acid (**18**)*. Yield 66%; mp 193-195 °C; 3288 (NH), 3066, 2983, 2858, 2692 (CH's), 1732, 1700 (C=O), 1624 (CN), 1519, 1346 (NO_2), 882, 673 (sust $_{1,2,4}$) cm^{-1}. ^1H NMR (300 MHz; DMSO-$_{d6}$/TMS): δ 1.24 (q, 2H, H_4, J = 8.7 Hz). 1.43 (q, 4H, $H_{3,5}$, J = 7.5 Hz), 2.16 (t, 4H, $H_{2,6}$, J = 7.2 Hz), 7.42 (s, 1H, H_{11}), 7.54 (d, 1H, H_{15}, J = 8.1 Hz), 7.74 (d, 1H, H_{14}, J = 8.1 Hz), 8.97 (s, 2H, $H_{8,9}$, NH). ^{13}C NMR (75 MHz, DMSO-$_{d6}$/TMS): δ 24.3 $C_{3,5}$, 28.2 C_4, 33.7 $C_{2,6}$, 99.4 C_{11}, 100.4 C_{15}, 120.8 C_{13}, 130.4 C_{14}, 147.0 C_{12}, 156.2 C_{10}, 171.8 C_7, 172.5 C_1. HRMS (DART [+1]) Found: 311.12770, calcd for $C_{13}H_{18}N_4O_5$ 311.12795.

References

1. Lang, D. K., Kaur, R., Arora, R., Saini, B. & Arora, S. **(2020)**. Nitrogen-containing heterocycles as anticancer agents: an overview, *Anti-Cancer Agents in Medicinal Chemistry*. 20, 2150-2168. 10.2174/1871520620666200705214917.
2. Alam, M. A. **(2023)**. Pyrazole: an emerging privileged scaffold in drug discovery. *Future Medicinal Chemistry*. 15, 21. https://doi.org/10.4155/fmc-2023-0207.
3. (a) Penieres-Carrillo, *et al*. **(2020)**. Reevaluating the synthesis of 2,5-disubstituted-1*H*- benzimidazole derivatives by different green activation techniques and their biological activity as antifungal and antimicrobial inhibitor, 57, 1, 436-455. https://doi.org/10.1002/jhet.3801.; (b) Ríos-Guerra, H. *et al.* **(2022)**. Household infrared technology as an energy-efficient approach to achieve C-Cπ bond construction reactions. *J. Braz. Chem. Soc*. 33, 1, 60-73. https://dx.doi.org/10.21577/0103-5053.20210124.
4. Cloc, R. C., Ruijter, E. & Orru, R. V. A. **(2014)**. Multicomponent reactions: advanced tools for sustainable organic synthesis. *Green Chem*. 16, 2958-2975. https://doi.org/10.1039/C4GC00013G.
5. (a) Abed, H. B., Mammoliti, O., Bande, O.; Lommen, G. V, & Herdewijn, P. **(2013)**. Strategy for the Synthesis of Pyridazine heterocycles and their derivatives. *J. Org. Chem*. 78, 7845−7858. https://doi.org/10.1021/jo400989q. (b) Li, X., Yu, Y. & Tu, Z. **(2021)**. Pyrazole scaffold synthesis, functionalization, and applications in Alzheimer's disease and Parkinson's disease treatment (2011–2020), *Molecules*, 26, 1202. https://doi.org/10.3390/molecules26051202. (c) Alam, M. A. **(2022)**. Antibacterial pyrazoles: tackling resistant bacteria, *Future Med. Chem*. 14, 343–362. https://doi.org/10.4155/fmc-2021-0275. (d) Nagwade, R. R., Khanna, V. V., Bhagwat, S.S. & Shinde, D.B. **(2005)**. Synthesis of new series of 1-Aryl-1,4-dihydro-4-oxo-6-methyl pyridazine-3-carboxylic acid as potential antibacterial agents. *Eur. J. Med. Chem.* 40, 1325-1330. https://doi.org/10.1016/j.ejmech.2005.05.012. (e) Sivakumar, R., Anbalagan, N., Vedachalam, G. & Joseph, T. L. **(2003)**. Synthesis and Anticonvulsant Activity of Novel 1-Substituted-1,2-dihydro-pyridazine-3,6-diones. *Biol. Pharm. Bull*. 26, 1407-1411. https://doi.org/10.1248/bpb.26.1407.
6. (a) Singh, S. P., Kumar, D., Jones, B. G. & Threadgill, M. D. **(1999)**. Formation and dehydration of a series of 5-hydroxy-5-trifluoromethyl-4,5-dihydropyrazoles. *Journal of Fluorine Chemistry*. 94, 199-203. https://doi.org/10.1016/S0022-1139(99)00011-1., (b) Sentezlenmesi, B. Y. P. **(2017)**. Synthesis of some new Pyrazoles. *Karaelmas Fen ve Müh. Derg.* 7, 352-355. http://fbd.beun.edu.tr.
7. Tierney, J. P. & Lidström, P. **(2007)**. Microwave-assisted organic synthesis, Blackwell Publishing Ltd, ISBN 978-1-4051-7590-6.
8. Hansen, T., Vermeeren, P., Bickelhaupt, F. M. & Hamlin, T. A. **(2021)**. Origin of the α-Effect in S_N2 Reactions. *Angew. Chem. Int. Ed*. 60, 20840–20848. https://doi.org/10.1002/anie.202106053.
9. a) Blake, J. F., Lim, D. & Jorgensen, W. L. **(1994)**. Enhanced hydrogen bonding of water to Diels-Alder transition states. Ab Initio evidence, *J. Org. Chem*. 59, 803-805. https://doi.org/10.1021/jo00083a021. (b) Rideout, D. C. & Breslow, R. **(1980)**. Hydrophobic Acceleration of Diels-Alder Reactions. *J. Am. Chem. Soc.* 102, 26, 7816-7817. https://doi.org/10.1021/ja00546a048.
10. Hu, Q., *et al*. **(2021)**. Microwave technology: a novel approach to the transformation of natural metabolites. *Chin Med*. 16, 87, 1-122. https://doi.org/10.1186/s13020-021-00500-8.
11. Juaristi, E. *et al*. **(2017)**. Stereoelectronic Interactions as a Probe for the Existence of the Intramolecular α-Effect. *J. Am. Chem. Soc*. 139, 10799−10813. https://doi.org/10.1021/jacs.7b05367
12. Mikołaj, S. and Karolina K. **(2024)** Nitro-functionalized analogues of 1,3-Butadiene: An overview of characteristic, synthesis, chemical transformations and biological activity. *Current Chemistry Letters.* 13, 15-30. https://doi.org/10.5267/j.ccl.2023.9.003.